magnetochemistry

MDPI

Article

Electrospun PCL/PVA Coaxial Nanofibers with Embedded Titanium Dioxide and Magnetic Nanoparticles for Stabilization and Controlled Release of Dithranol for Therapy of Psoriasis

Natália Andrýsková [1], Paul Sourivong [2], Melánia Babincová [3,*], Peter Babinec [3] and Mária Šimaljaková [1]

[1] Department of Dermatovenereology, Faculty of Medicine, Comenius University and Bratislava University Hospital, Mickiewiczova 13, 813 69 Bratislava, Slovakia; babincova15@uniba.sk (N.A.); maria.simaljakova@sm.unb.sk (M.Š.)
[2] Department of Radiation Oncology, Houston Methodist San Jacinto Hospital, 4021 Garth Road, Suite 105, Baytown, TX 77521, USA; sourivong@hotmail.com
[3] Department of Nuclear Physics and Biophysics, Faculty of Mathematics, Physics and Informatics, Comenius University, Mlynská dolina F1, 842 48 Bratislava, Slovakia; babinec@fmph.uniba.sk
* Correspondence: melania.babincova@fmph.uniba.sk

Abstract: Dithranol is one of the oldest and most efficient drugs used in the treatment of psoriasis. One of the challenges with using dithranol is its photostability, because it easily degrades when exposed to light. This study investigated the potential of coaxial core-sheath PCL/PVA nanofibers as a dual-functional system for enhancing dithranol photostability and remote-controlled drug delivery for psoriasis therapy. We have shown that coaxial nanofibers with titanium oxide nanoparticles (reflecting and absorbing ultra-violet light) in the PVA-based sheath part of the nanofibers can increase dithranol photostability. Incorporation of dithranol and magnetic nanoparticles into a PCL-based core of the nanofibers enables dithranol release control via an external radio-frequency field. The application of a radio-frequency field generates heat that can be used to control the release rate of drugs. Our approach therefore offers a non-invasive and remotely controlled drug release system that hold promise for the development of new topical formulations for psoriasis treatment using dithranol.

Keywords: psoriasis; magnetic nanoparticles; photostability; dithranol; coaxial nanofibers

Citation: Andrýsková, N.; Sourivong, P.; Babincová, M.; Babinec, P.; Šimaljaková, M. Electrospun PCL/PVA Coaxial Nanofibers with Embedded Titanium Dioxide and Magnetic Nanoparticles for Stabilization and Controlled Release of Dithranol for Therapy of Psoriasis. *Magnetochemistry* **2023**, *9*, 187. https://doi.org/10.3390/magnetochemistry9070187

Academic Editor: Alejandro Gómez Roca

Received: 15 May 2023
Revised: 12 July 2023
Accepted: 17 July 2023
Published: 19 July 2023

1. Introduction

Psoriasis is a multifactorial, genetically conditioned, chronic, relapsing immune-based disease with a variable clinical picture, which is characterized by a non-physiological reaction of the epidermis to the effects of various provocative factors from the external and internal environment [1,2]. A typical clinical manifestation of psoriasis is an erythemato-squamous deposit, which reflects the pathogenesis of this disease, specifically inflammation and hyperproliferation. Both phenomena are the result of the interaction of the innate and acquired immune systems. T lymphocytes and the cytokines produced by them play a key role. In predisposed individuals, the cells of the innate immune system (keratinocytes, plasmacytoid dendritic cells, macrophages, and NK T lymphocytes) are activated by an unknown antigen. This results in the production of cytokines (tumor necrosis factor alpha, interferon alpha, interferon gamma, interleukin-1 beta, interleukin-6) that activate myeloid dendritic cells. These activated cells present antigens and produce cytokines from the group of interleukins, including IL-12 and IL-23, which subsequently leads to the differentiation of T lymphocytes into subgroups Th1 and Th17. These differentiated T lymphocytes produce interleukin-17A, interleukin-17F, and interleukin-22, which activate keratinocytes and induce the production of antimicrobial peptides and pro-inflammatory cytokines, which maintain the inflammatory process in an active phase [3–5]. The goal of treatment is to put psoriasis into remission and keep it in this state for as long as possible [6]. The PASI score (psoriasis area and severity index) is most often used to assess the severity, where

a range of 0 to 72 points is possible [7]. Another parameter used is BSA (body surface area: percentage extent of skin surface involvement), where a range from 0% to 100% is possible. Patients with moderate and severe psoriasis, defined as patients with a PASI score above 10 and a BSA above 5%, require total treatment [8]. With the introduction of biologics, great progress has been made in the systemic treatment of psoriasis. Therapy with antibodies against IL-17 or IL-23 leads to almost complete clinical clearance of psoriatic lesions. Approximately 70–80% of patients with psoriasis have a mild-to-moderate form [9], in which local treatment has mostly sufficient therapeutic efficacy and has fewer potential side effects compared to general treatment. Modern local treatment requires not only new, effective substances but also improved galenic formulations [10–12].

Nanocarriers such as nanoparticles offer several advantages over conventional therapies.

Firstly, nanocarriers can be designed to target specific cells or tissues, allowing for precise drug delivery. By delivering the drug in proximity to the target cells, nanocarriers increase the therapeutic benefits while minimizing the side effects on healthy cells.

Furthermore, nanoparticles can improve the bioavailability of the drug. Their small size and large surface area-to-volume ratio facilitate efficient absorption and uptake by the skin. This enhanced bioavailability ensures that a higher proportion of the drug reaches the target site, increasing its efficacy.

Additionally, nanocarriers provide protection for the drug, shielding it from degradation and biodegradation. This protection helps maintain the stability of dithranol, preserving its potency and extending its shelf life.

Controlled drug release is another advantage of nanocarriers. Their unique properties allow for the controlled release of the drug in the desired concentrations over an extended period. This controlled release ensures a sustained therapeutic effect and reduces the frequency of administration.

Overall, incorporating antipsoriatic drugs into nanocarriers offers a modern and effective approach for psoriasis treatment. It enhances drug delivery, improves bioavailability, protects the drug, and enables controlled release, all of which contributes to improved therapeutic outcomes and minimizes side effects [13–18].

Dithranol (Figure 1a), known also as cignoline or anthralin (1,8-Dihydroxy-9(10H)-anthracenone), is a synthetic derivative of chrysarobin (Figure 1b), a natural product from the bark of the South American araroba tree, used since 1916 [19] as a topical treatment for psoriasis. Dithranol reduces the proliferation of keratinocytes and the activation of T lymphocytes and regulates cell differentiation, probably by its accumulation in mitochondria and the production of reactive oxygen species (ROS), inducing apoptosis [20–26]. While dithranol's lipophilic nature and ability to penetrate the skin quickly are advantageous for its therapeutic use, they can also lead to some of its unwanted side effects; for example, skin irritation and skin and laundry staining [27]. In addition, factors such as poor solubility, poor stability, and toxicity hamper its use as a potential therapeutic agent. Dithranol is easily oxidized by light, metal ions, and oxygen, and forms reactive oxygen species as intermediates during oxidation. Dithranol metabolites such as anthraquinone and dithranol dimer (Figure 1c–d) have been detected in human and rat skin. Dithranol also forms ether-insoluble products in intact skin, which are chemically less well characterized but may contain polycyclic aromatic hydrocarbons. However, the development of novel drug delivery technologies and modifications to the molecular structure of dithranol can help to address these issues and enhance its therapeutic potential.

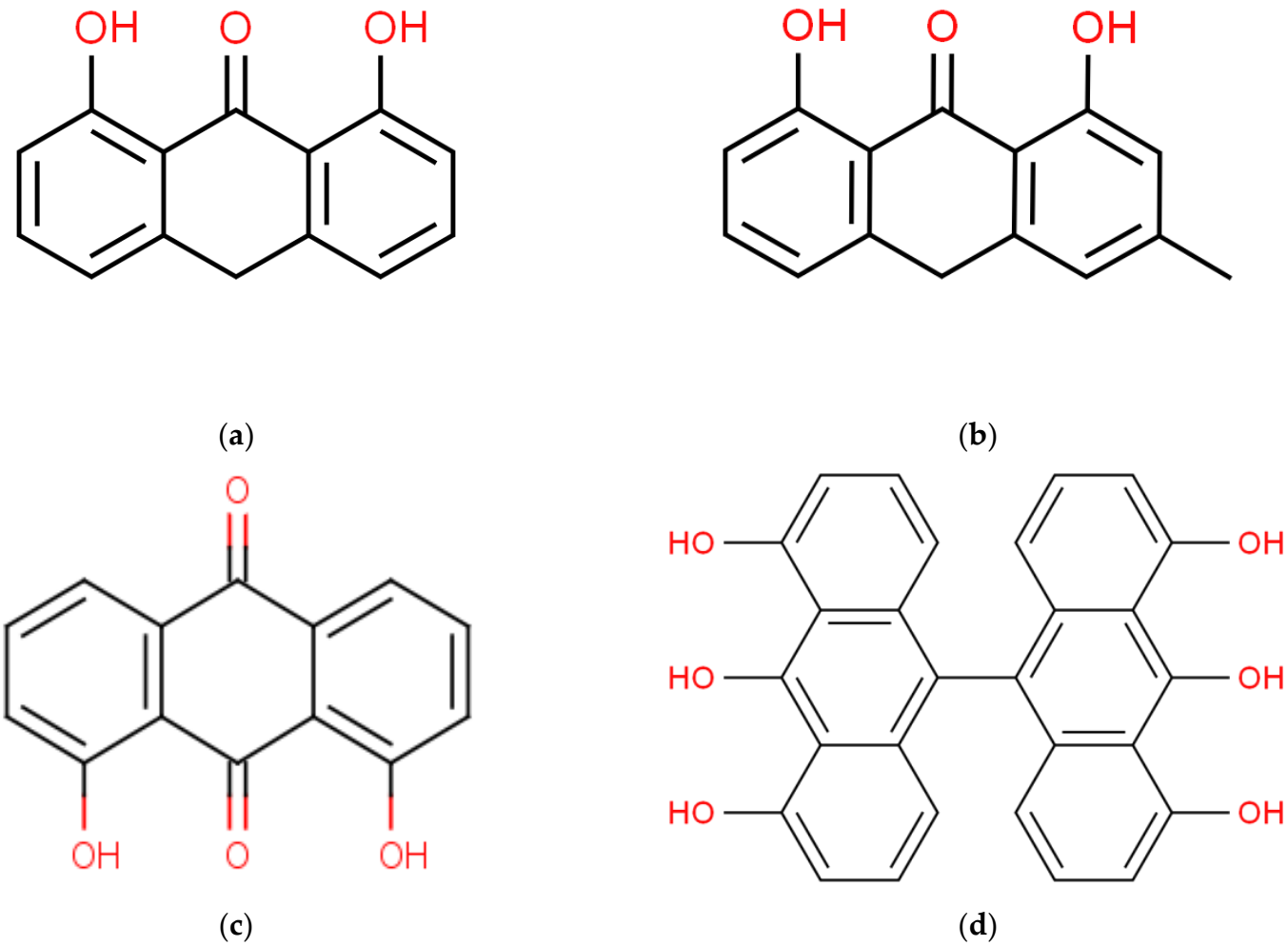

Figure 1. Structures of (**a**) dithranol (1,8-Dihydroxy-9(10H)-anthracenone); (**b**) chrysarobin (1,8-Dihydroxy-3-methyl-9(10H)-anthracenone); (**c**) danthron (1,8-Dihydroxy-9,10-anthracenedione); and (**d**) dithralon dimer (10-(4,5,10-trihydroxyanthracen-9-yl) anthracene-1,8,9-triol).

These technologies include dendrimers [28], nanoemulsions [29], nanostructured lipid gels [30], liposomes [31], polymer-based nanoparticles [32], and niosomes [33,34]. These technologies can improve the solubility and stability of dithranol, reduce skin irritation, and target the drug to specific sites of the body, thereby reducing the risk of systemic toxicity. In addition to these drug delivery technologies, other approaches such as combining dithranol with other medications (for example, salicylic acid [35]), using it in combination with phototherapy [36], and modifying the molecular structure or mode of action [37,38] of dithranol have been investigated to improve its therapeutic potential. These strategies can help to address the limitations of dithranol and make it a more effective and safe treatment option for psoriasis and other skin disorders [39,40].

This paper specifically aims to use electrospun nanofibers for the photoprotection and controlled delivery of dithranol. Electrospinning is a process used to create ultrafine fibers, typically with diameters in the range of a few nanometers to several micrometers. It involves the use of an electric field to stretch and draw a polymer solution into a thin fiber. The process is commonly used in materials science, biomedicine, and other fields to create materials with unique properties for improving the therapy of psoriasis [41,42], including using drugs such as calcipotriol and tazarotene [43], tazarotene and magnetic nanoparticles [44], nanofiber-mediated hyperthermia [45], methotrexate and hyperthermia [46], and tretinoin [47]. The electrospinning process can be modified to create fibers with different shapes, sizes, and properties by varying factors such as the polymer composition, flow rate,

electric field intensity, and collector plate design. It is a versatile and scalable technique that has many potential applications in fields such as tissue engineering, drug delivery, and energy storage. More specifically, we have used coaxial electrospinning, a process in which two concentric spinnerets can receive two different polymers. The coaxial electrospinning process has several advantages over traditional electrospinning. First, it allows the production of nanofibers with a core-sheath structure, which can have unique properties and applications in various fields such as drug delivery, tissue engineering, and energy storage. Second, it enables the encapsulation of different materials within the nanofibers, such as drugs [48], hydroxyapatite [49], and enzymes or nanoparticles, which can be released at a controlled rate [50–52].

Solar radiation (280–800 nm) is a natural agent creating the earth's climate and has a significant impact on the environment. The ultraviolet part of the solar spectrum (UV) plays an important role in many processes taking place in nature, especially in the biosphere [53,54]. It has several positive and desirable effects, but when "safe" values are exceeded it can often have harmful effects. Depending on the type of protective filter, photoprotection can be divided into chemical (absorbers) and physical (blockers). Physical methods used in the context of sunscreens and UV protection often rely on the principle of reflecting the sun's rays. These methods take advantage of materials such as titanium dioxide (TiO_2), which acts as a reflective surface resembling numerous tiny mirrors.

Titanium dioxide is a commonly employed ingredient in the formulation of sunscreens and various other products intended to offer protection against ultraviolet radiation. When applied to the skin, titanium dioxide particles scatter and reflect UV radiation, preventing it from reaching the deeper layers of the skin. This mechanism aids in reducing the harmful effects of UV radiation, including sunburn and long-term skin damage. The reflective properties of titanium dioxide are attributed to its high refractive index and ability to efficiently scatter and reflect UV light. The particles of titanium dioxide act as physical barriers, redirecting the incident UV rays away from the skin's surface. By incorporating titanium dioxide into sunscreen formulations or other UV-protective products, manufacturers can enhance their effectiveness in shielding the skin from harmful UV radiation. This physical protection complements other methods, such as the absorption of UV radiation by chemical filters, to provide comprehensive sun protection [54–58]. TiO_2 has a high refractive index, which enables it to scatter and reflect UV radiation, thus providing effective UV protection. In addition, TiO_2 has a wide bandgap and can absorb UV radiation, leading to the formation of electron-hole pairs, which can act as reactive species that can degrade harmful compounds. Our aim in this study was the fabrication of electrospun coaxial nanofibers which contain TiO_2 nanoparticles in the outer sheath part for UV protection and magnetic nanoparticles embedded in the inner core part for remote-controlled dithranol release at the desired times and quantities using an external radio-frequency field.

2. Materials and Methods

2.1. Materials

Dithranol (99%), Polycaprolactone (PCL, Figure 2a) (molecular weight = 80,000), Polyvinyl alcohol (molecular weight = 80,000–100,000) (PVA, Figure 2b), Titanium dioxide nanoparticles with dimension 30 nm, and other chemicals and material were obtained from Sigma-Aldrich company (Saint Louis, MO, USA) unless otherwise stated. PCL-stabilized magnetic nanoparticles (MN) were prepared according to [59]. Crude magnetic nanoparticles were then prepared by precipitation from a single iron precursor in a controlled oxidative environment; the magnetic nanoparticles were further functionalized with a double-layered cationic CTAB surfactant to enhance their stability and provide proper surface functionality for biopolymer conjugation through electrostatic interactions. Following this, the CTAB-coated SPIONs were applied as a core and coated with a thin layer of PCL biopolymer through the "graft-to" approach to achieve enhanced cytocompatibility and physicochemical properties.

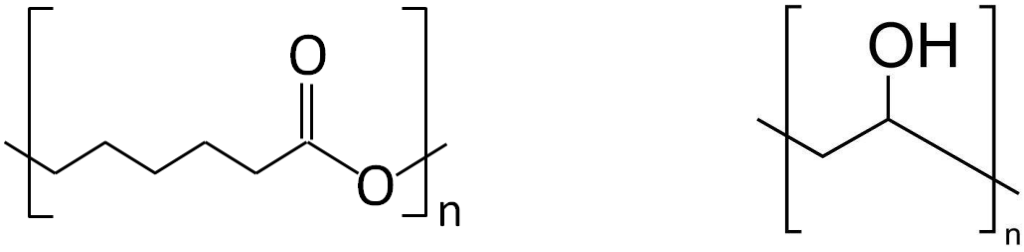

(**a**) (**b**)

Figure 2. Structures of (**a**) polycaprolactone PCL and (**b**) polyvinyl alcohol PVA polymers used for electrospinning of coaxial nanofibers.

2.2. Coaxial Electrospinning Process

PCL 10% (*w*/*v*) solution was prepared by dissolving 10 g of PCL in 10 mL of chloroform:acetone (7:3, *v*/*v*) mixture at 50 °C for formation of the core structure of the nanofibers with PCL-stabilized MN and dithranol in the desired concentrations. The PVA solution was prepared by dispersing 30 nm TiO_2 nanoparticles in PVA 8% (*w*/*v*) water solution to form the sheath contents of the nanofibers. Coaxial electrospinning was performed using a custom-made coaxial nozzle. The prepared [(Dithranol&MN)@PCL] (for core) and [(TiO_2)@PVA] (for sheath) solutions were uploaded to the pumps. The coaxial needle used in this process was of gauge 17 for PVA the sheath and gauge 23 for the PCL core. The flow of polymers through the coaxial needle was driven by two Terumo TE-331 syringe pumps (Terumo, Shibuya, Japan) both using a flow rate of 0.7 mL h^{-1}. A 15 kV voltage was applied to the needle from the DC supply. The distance from the needle to the drum collector was 13 cm (Figure 3). Nanofibers were also deposited onto aluminum foil, or directly onto the skin surface.

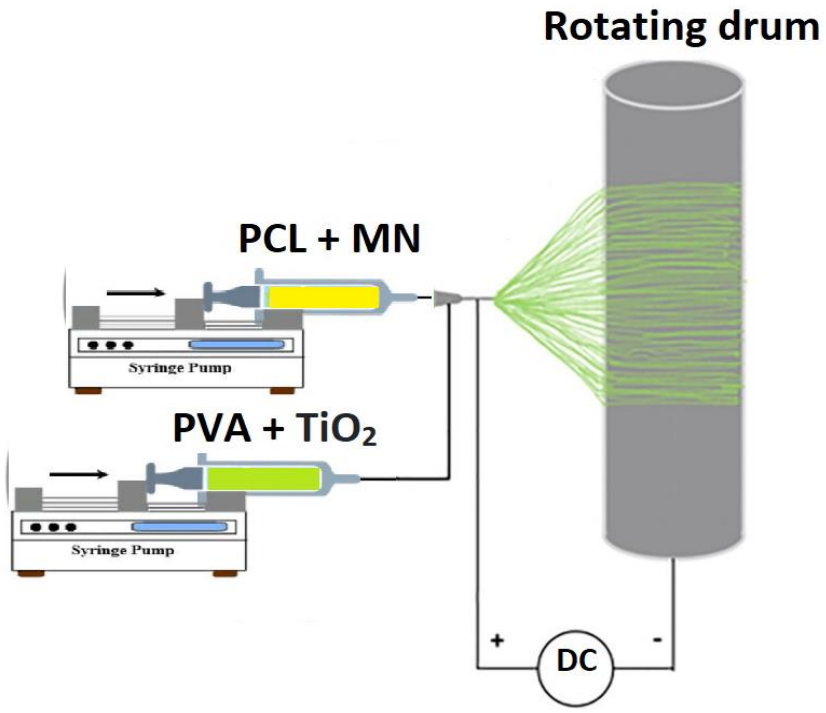

Figure 3. Coaxial electrospinning of functionalized polycaprolacton/polyvinyl alcohol core-sheath nanofibers.

2.3. Study of the Morphology and Structure of the Nanofibers

A scanning electron microscope (SEM) was used to obtain images of the nanofibers using Tescan, Lyra3 (Brno, Czech Republic) equipment. Nanofiber fabrics were covered with a 20 nm layer of platinum and gold (20:80) before imaging. The secondary electron emission mode was used with a voltage of 10–30 kV at a distance of 15 mm for image acquisition. This technique allows for high-resolution imaging of the nanofibers, providing information on their morphology, structure, and composition. The SEM images obtained can help to understand the properties of the nanofibers and can be used to optimize their production and performance in various applications. The nanofiber diameter distribution was estimated using two methods: the UTHSCSA ImageTool for Windows freeware and manual measurement of individual diameters across the image [60]. The UTHSCSA ImageTool 3.0 is a piece of software that allows for the analysis of digital images, and in this case it was used to measure the diameters of the nanofibers. The manual measurement method involved measuring the diameters of individual nanofibers across the image (for each sample the diameter distribution was evaluated from 100 measurements of randomly chosen nanofibers).

2.4. Application of the Radio-Frequency Field (RF) for Nanofiber Heating

To generate electromagnetic radiation with a frequency of 1.75 MHz, we used a customized, water-cooled, high-frequency generator GV6A (ZEZ, Rychnov u Jablonce nad Nisou, Czech Republic), the components of which are shown in Figure 4.

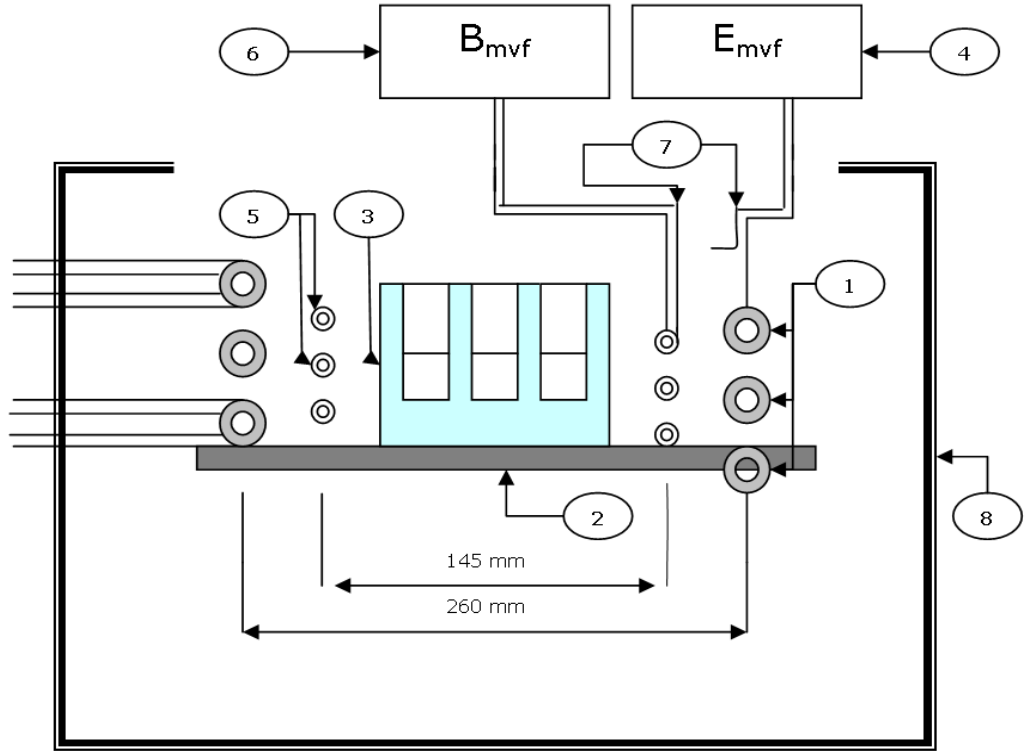

Figure 4. Schematic representation of a customized GV6A radio-frequency generator apparatus: The apparatus includes the following components: (1) three-turn induction copper coil (diameter 24 mm) of the resonant circuit cooled by water; (2) supporting Teflon plate; (3) measured samples thermally insulated with polystyrene foam; (4) HF voltage amplitude meter; (5) induction copper thread (diameter 0.7 mm); (6) VF magnetic field induction meter; (7) high voltage wires (15 kV) connected to E_{mvf} and B_{mvf}; (8) grounded shell or conductive plate of the capacitor.

The technical parameters of the HF generator were:

- maximum voltage on the resonance coil U_{mvf} = 4.5 KV;
- maximum power P_{mvf} = 6 kW (P_{mvf} and U_{mvf} can be regulated);
- maximum input P_{max} = 10 kVA;
- magnetic induction B = 1.13 mT.

The temperature was measured using a UT303+ contactless thermometer (UNI-T, Shanghai, China).

2.5. Determination of Magnetic Properties

To measure the saturation magnetization of the nanofiber samples we used a MicroMag TM3900 (Princeton Measurements Corp., Westerville, OH, USA) VSM magnetometer. The saturation magnetization is the maximum magnetization that a material can achieve in a magnetic field, and it provides important information about the magnetic behavior of the material. A vibrating sample magnetometer is a widely used instrument for measuring the magnetic properties of diverse materials, and it can measure the characteristic magnetism of a sample with high accuracy and precision.

2.6. Dithranol Controlled Release

The release of dithranol from a nanofiber patch with dimensions of 1 cm × 3 cm was investigated using the dialysis bag method. Since dithranol has very limited solubility in aqueous media (less than 0.2 mg/mL), a citrate buffer containing 20% methanol and 1% sodium lauryl sulphate was used as the release medium.

To conduct the experiment, aliquots of dithranol-containing nanofiber patches were introduced into a dialysis tube with a molecular weight cutoff (MWCO) of 3.5–5 kDa. The dialysis tube acted as a semi-permeable membrane, allowing the passage of the released dithranol while retaining the nanofibers. The dialysis tube containing the solution was then immersed in 30 mL of the release media. At specific time intervals, aliquots of the release media were taken, and an equal volume of fresh release medium was added to maintain sink conditions. Sink conditions ensured that the concentration of the released compound in the release media remained much lower than its solubility limit, facilitating accurate measurements. The concentration of released dithranol was determined using a UV MINI 1240 UV–VIS spectrophotometer (Shimadzu, Kyoto, Japan) at a wavelength of 375 nm, according to the calibration curve shown in Figure 5b. Information about the release profile of dithranol from the nanofiber patch was obtained by analyzing the concentration of dithranol released over time.

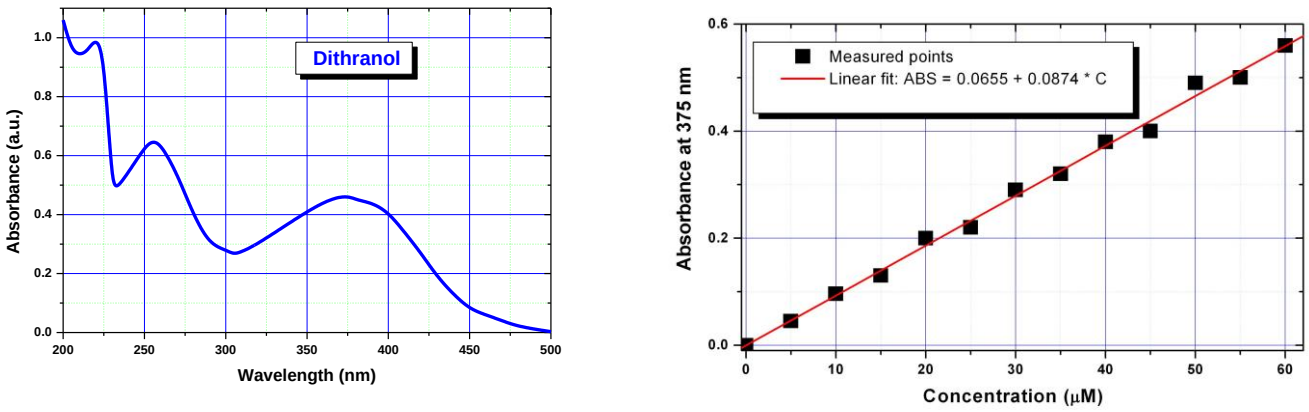

(**a**) (**b**)

Figure 5. (**a**) UV-VIS absorption spectra of dithranol in chloroform/acetone; (**b**) calibration curve of dithranol at wavelength 375 nm.

2.7. Quantification of Dithranol Photodegradation

Photodegradation studies of dithranol were conducted using a TL-D/08 Blacklight Blue UVA lamp, which is a 36 W low-pressure mercury-vapor fluorescent lamp (Philips, Eindhoven, The Netherlands). To perform the experiment, samples of dithranol in various formulations were placed in UV-transparent quartz cuvettes and exposed to UVA light in a closed chamber. Individual cuvettes were used for each regular time interval in our experimental setup, with one measurement taken per hour. This approach allowed the tracking of changes in the amount of dithranol over time.

To quantify the amount of remaining dithranol, a cuvette was withdrawn at each time interval containing a sample of the reaction mixture. The cuvette was then evaluated, presumably through a measurement or analysis technique, to determine the remaining amount of dithranol.

This methodology enables the monitoring the degradation or consumption of dithranol over time and provides an insight into the kinetics or dynamics of the process under investigation. By assessing the amount of remaining dithranol in each cuvette, one can potentially observe trends or patterns in its concentration over the course of the experiment [61].

2.8. Statistical Analysis

All experiments were prepared and analyzed at least in triplicate to ensure the reliability and reproducibility of the results. The data obtained from the experiments are expressed as mean ± SD (standard deviation). To compare the experimental data and assess the statistical significance of any differences, a one-way analysis of variance (ANOVA) was employed (significance level of 5).

3. Results and Discussion

The effectiveness of TiO_2 in providing UV protection depends on several factors, including the particle size, concentration, and crystal structure of the TiO_2 used. Smaller TiO_2 particles have a higher surface area and can provide better UV protection, while higher concentrations of TiO_2 can also enhance the effectiveness of UV protection. The crystal structure of TiO_2 can also influence its UV protection capabilities, with the anatase form being more effective than the rutile form. In addition to its UV protection capabilities, TiO_2 also has other beneficial properties, such as its antimicrobial activity, self-cleaning properties, and catalytic activity.

Many drugs, including dithranol, can be sensitive to light and undergo degradation when exposed to UV radiation. This can result in loss of potency and altered effectiveness of the drug, which may reduce its therapeutic benefits and potentially cause adverse effects.

To protect dithranol from UV radiation, a similar principle to that used in sunscreens can be applied. Titanium dioxide nanoparticles are known as UV light blockers or UV filters. These nanoparticles can absorb and scatter UV radiation, thereby reducing the amount of UV light that reaches the drug. By incorporating TiO_2 nanoparticles into the formulation containing dithranol, the nanoparticles act as a protective shield, minimizing the exposure of dithranol to harmful UV radiation.

This approach helps to enhance the photostability of dithranol by preventing or reducing the chemical reactions that occur when the drug is exposed to UV light. By incorporating TiO_2 UV light blockers, the formulation can provide a protective barrier against UV radiation, maintaining the potency and efficacy of dithranol over a longer period.

For the purposes of dithranol photostabilization [62–65], we prepared the coaxial nanofiber with a core-sheath structure [(Dithranol&MN)@PCL]/[TiO_2@PVA] which consists of two distinct layers (Figure 6). The core layer is composed of a mixture of the hydrophobic drug dithranol and PCL-covered magnetic nanoparticles embedded in the PCL polymer matrix. The sheath layer is composed of TiO_2 nanoparticles embedded in PVA (the polyvinyl alcohol polymer matrix which serves as a UV blocker protecting the dithranol in the core). When TiO_2 is included in a sheath layer, it acts as a physical barrier

that prevents UV radiation from reaching the drug in the core. This helps to ensure that the dithranol remains stable and effective over time. The coaxial structure allows for the remote-controlled release of dithranol from the core layer under the control of a radio-frequency field, as demonstrated in our laboratory already in 1993 [66] and then widely developed and applied [67–72]. In the case of polycaprolactone (PCL)/polyvinyl alcohol (PVA) core-sheath nanofibers, PCL was used as the core material and PVA as the sheath material. PCL is a biodegradable polyester with good mechanical properties, while PVA is a water-soluble polymer with good biocompatibility. The combination of PCL and PVA in core–shell nanofibers can create a material with improved mechanical strength and biocompatibility. PCL/PVA coaxial nanofibers exhibit enhanced mechanical properties compared to individual PCL or PVA nanofibers. The PCL core provides higher tensile strength and stiffness, while the PVA shell layer improves the toughness of the nanofibers [73]. The cytotoxicity, biocompatibility, and degradation rate of PCL have been widely studied in short- and long-term nanofiber implantations [74,75] and PVA is highly biodegradable and biocompatible [76].

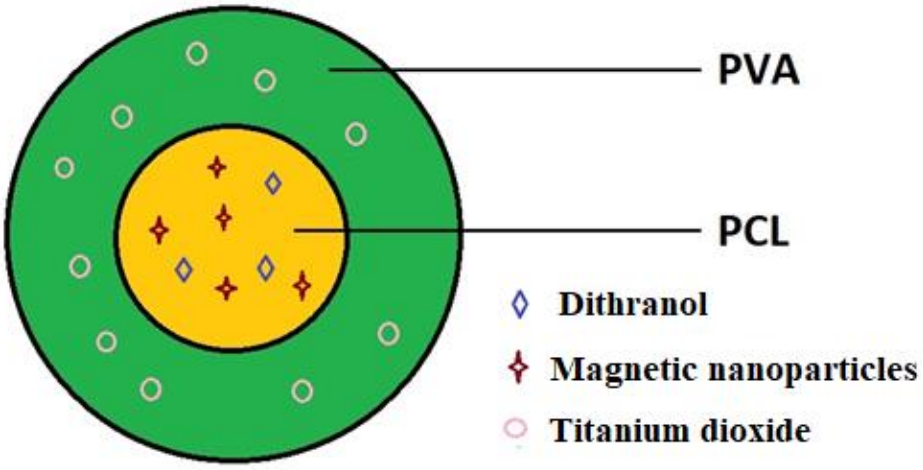

Figure 6. Schematic structure of core-sheath coaxial nanofibers [(Dithranol&MN)@PCL]/TiO_2@PVA].

The structure and morphology of [(Dithranol&MN)@PCL]/[TiO_2@PVA] nanofibers, as observed using SEM, is shown in Figure 7a, together with the distribution of nanofiber diameters (Figure 7b). The fabricated nanofibers had a Gaussian distribution of diameter from 200 to 900 nm, with mean diameter close to 500 nm and a uniformly smooth surface structure [77].

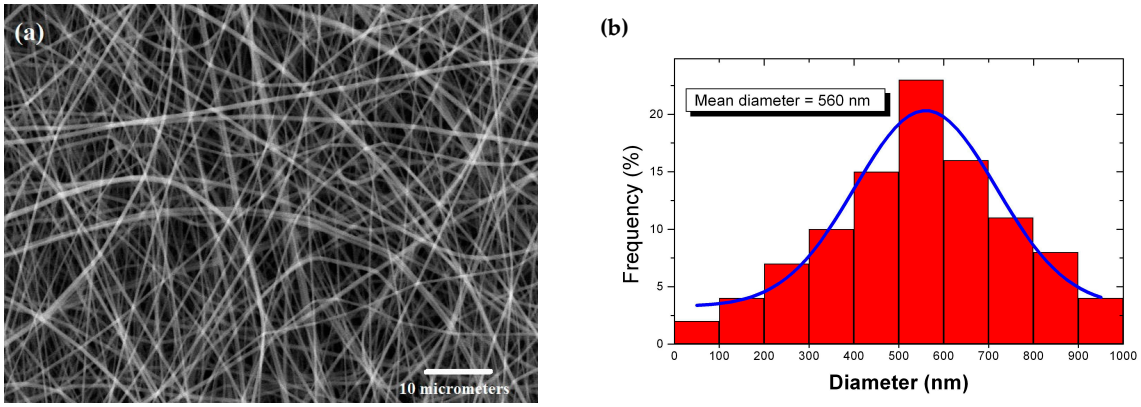

Figure 7. (**a**) Morphology of nanofibers from scanning electron microscopy; (**b**) distribution of nanofiber diameters.

The magnetization curve of the nanofibrous mat (Figure 8) indicates a saturation magnetization value of approximately 3.9 emu/g when exposed to an external magnetic field.

It can also be observed that the magnetization does not saturate, even at an external field strength as large as 10,000 A/m. These findings are indicative of the superparamagnetic behavior of the system. Superparamagnetism [78] is a phenomenon that occurs in small magnetic particles where thermal energy can overcome the magnetic anisotropy energy barrier, leading to fluctuations in the magnetization direction. As a result, superparamagnetic particles do not exhibit a permanent magnetic moment, and their magnetization can be switched by applying an external magnetic field, which is crucial for our application. PCL-coated magnetic nanoparticles have structural stability, uniform particle size, improved dispersity, cytocompatibility, and controlled heating under hyperthermia condition. Moreover, we embedded them into PCL nanofibers, which guarantees compatibility.

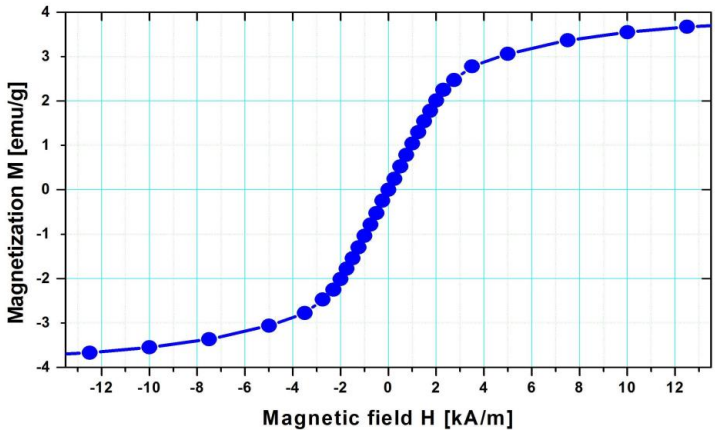

Figure 8. Magnetization of electrospun coaxial nanofiber fabric with 5 wt% of magnetic nanoparticles measured using VSM magnetometer.

After application of the RF field, the magnetic nanoparticles are efficiently heated up (Figure 9) and because the melting temperature of the PCL polymer is rather low (40–50 °C) the generated heat can be used to control the release rate of drugs (Figure 10). When the radio-frequency field is turned on, the produced heat softens or melts the PCL, allowing the dithranol to diffuse out. When the RF field is turned off, the PCL solidifies, trapping the drug inside [41].

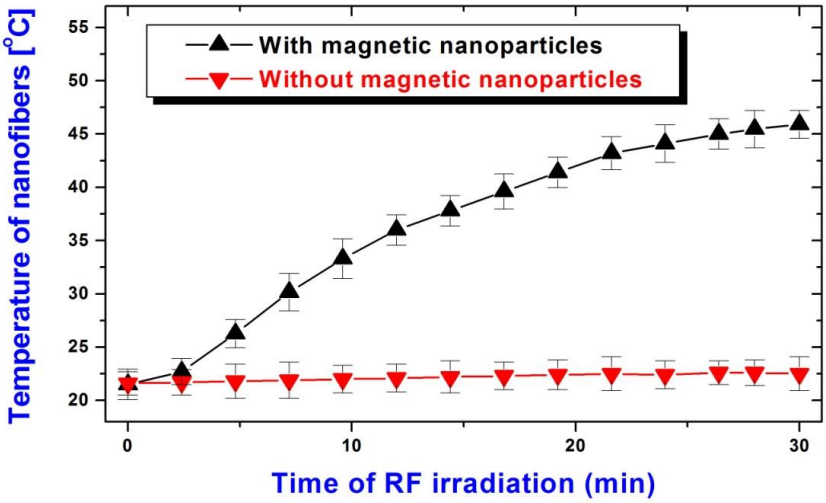

Figure 9. Heating of nanofiber mat in 1.75 MHz radio-frequency field (results from three independent experiments).

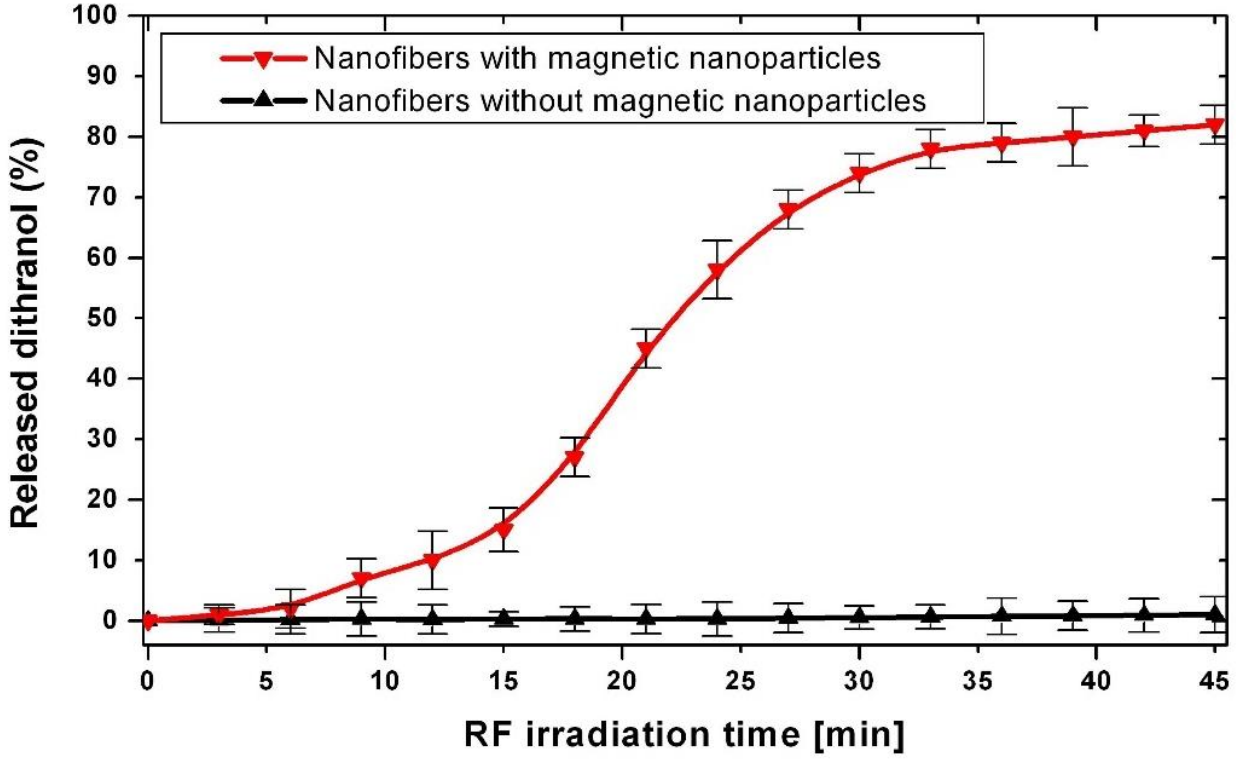

Figure 10. Release profile of dithranol form core-sheath [(Dithranol&MN)@PCL]/[TiO_2@PVA] nanofibers with and without magnetic nanoparticles co-embedded with dithranol in PCL core (results from three independent experiments).

In general, burst release is typical for drug release from nanofibers due to the large surface area-to-volume ratio of the nanofiber. Thanks to the fact that the medicine is encapsulated in a core part of the coaxial nanofiber, our approach avoids this unpleasant effect.

Moreover, heating may have a synergistic effect on psoriasis therapy. Specifically, the heat may increase the therapy's effectiveness by providing superficial hyperthermia. Superficial hyperthermia involves applying heat to the skin's surface, which can help improve blood circulation and lymphatic drainage. It may also increase drug permeability through the skin, making it more effective for treating psoriasis [79].

The excellent UV light-blocking property of TiO_2 fabric is attributed to the combined effect of its good absorption and strong scattering of UV light. The absorption and scattering properties of TiO_2 fabric provide excellent protection against harmful UV radiation. Figure 11 provides absorbance spectra in the UVA (315–400 nm) and UVB (290–315 nm) range.

Photodegradation experiments on non-stabilized dithranol formulations evidenced the very fast degradation of the drug. The dithranol residual concentration was 50% after just 10 h of illumination (Figure 12), corresponding to a radiant exposure of 130 kJ/m^2. In the next step, photodegradation studies were applied on novel formulations prepared by entrapping coaxial nanofibers which were was exposed to light as described above. The results showed a clear decrease in dithranol degradation, with a very impressive 96% residual concentration after 10 h of illumination for fabric containing TiO_2. It is interesting that even the specimen without TiO_2 was protected against UV degradation (80% residual content), which may be explained by the presence of PCL microcrystals reflecting and scattering UV radiation [62].

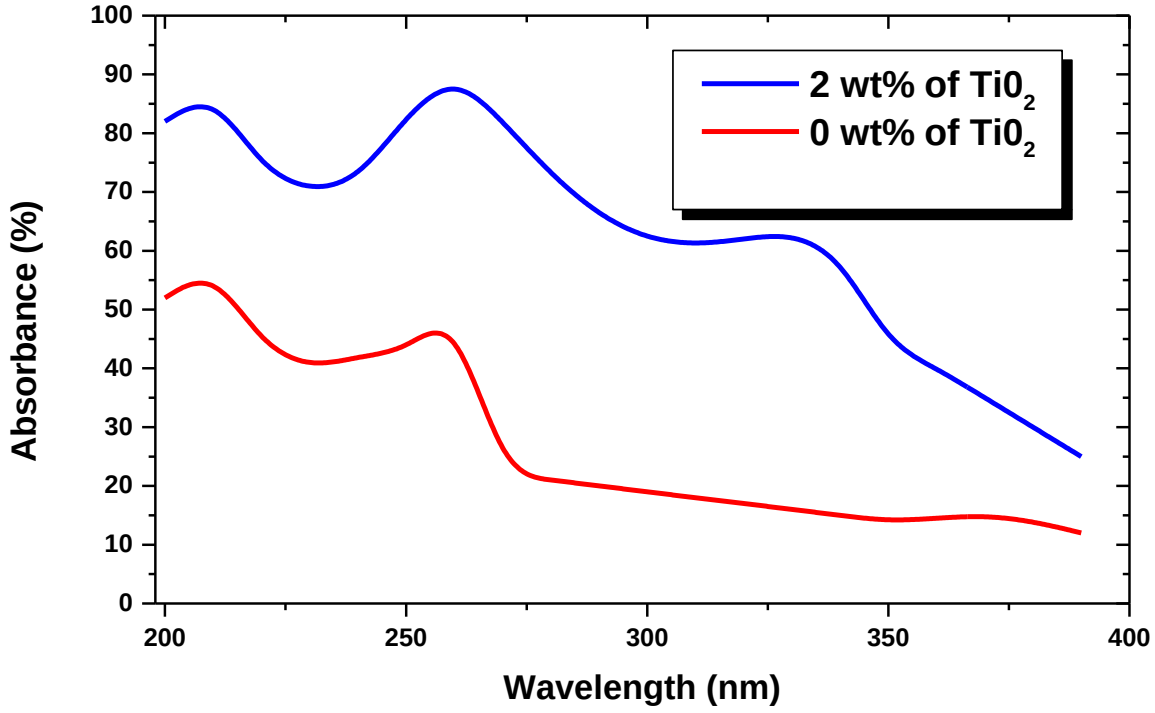

Figure 11. Absorbance spectrum of coaxial [(Dithranol&MN)@PCL]/[TiO_2@PVA] nanofiber mat with 2 wt% TiO_2 and without TiO_2 nanoparticles (results from three independent experiments).

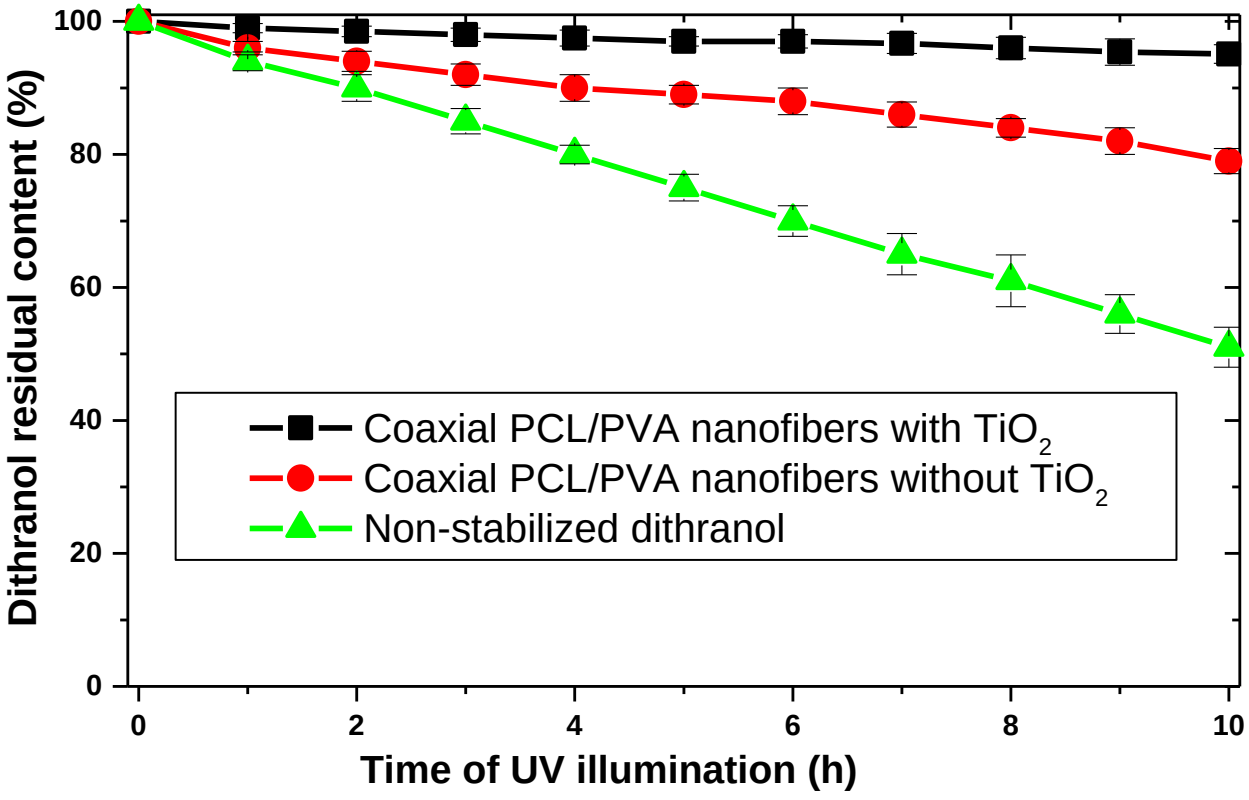

Figure 12. Dithranol residual content as a function of illumination time for non-stabilized dithranol and for coaxial PCL/PVA nanofibers with 2 wt% TiO_2 and without TiO_2 (results from three independent experiments).

4. Conclusions

Dithranol is known to degrade easily when exposed to light, which can reduce its effectiveness and shelf life. To address this issue, researchers have explored different strategies, including incorporating dithranol into various formulations such as nanofibers, liposomes, and microemulsions.

This study specifically investigated the use of coaxial nanofibers with titanium dioxide nanoparticles in the sheath part and magnetic nanoparticles in the core part. This combination aimed to enhance the photostability of dithranol while enabling controlled drug release through an external radio-frequency field. The presence of titanium dioxide nanoparticles in the sheath of the nanofibers helped to increase the photostability of dithranol by protecting it from degradation when exposed to light. Additionally, incorporating magnetic nanoparticles in the core allowed for non-invasive and remotely controlled drug release through the generation of heat by applying a radio-frequency field.

The findings suggest that the developed coaxial nanofibers hold promise for the development of new topical formulations for the treatment of psoriasis using dithranol. By improving the drug's photostability and enabling controlled release, this approach offers potential benefits in terms of effectiveness, shelf life, and convenience for patients.

Although we have used experimental equipment for the generation of a radio-frequency field, such a treatment has a long history of use in medicine. Initially, it was used for the burning of unwanted tissues, and over time its application has expanded to include neurosurgery and cardiac surgery. In 2002, the American FDA approved the first device (ThermaCool by Thermage, Bothel, WA, USA) that used monopolar RF for reducing wrinkles and rejuvenating skin. Subsequently, the Aluma device (Lumenis Ltd., Yokneam, Israel), which utilizes bipolar RF, was also approved by the FDA for similar purposes. Both monopolar and bipolar RF devices in cosmetic dermatology typically operate at frequencies of 1–10 MHz. These commercial and widely available certified instruments can be safely used also for the purposes of dithranol release using the presented method.

Author Contributions: Conceptualization, methodology, validation, formal analysis, investigation, and data curation, N.A., P.S., P.B., M.B. and M.Š.; writing—original draft preparation, N.A.; writing—review and editing, M.B., P.B. and M.Š. All authors have read and agreed to the published version of the manuscript.

Funding: This research was funded by the Slovak Grant Agency VEGA project No. 1/0639/22.

Institutional Review Board Statement: Not applicable.

Informed Consent Statement: Not applicable.

Data Availability Statement: Not applicable.

Conflicts of Interest: The authors declare no conflict of interest.

References

1. Kocaaga, A.; Kocaaga, M. Psoriasis: An Immunogenetic Perspective. *Glob. Med. Genet.* **2022**, *9*, 82–89. [CrossRef] [PubMed]
2. Simaljaková, M.; Buchvald, D. *Dermatovenereology*; Comenius University Press: Bratislava, Slovakia, 2019.
3. Griffiths, C.E.M.; Armstrong, A.W.; Gudjonsson, J.E.; Barker, J.N.W.N. Psoriasis. *Lancet* **2021**, *397*, 1301–1315. [CrossRef]
4. Buc, M. *Autoimunita a Autoimunitné Choroby*; VEDA: Bratislava, Slovakia, 2016.
5. Armstrong, A.W.; Read, C. Pathophysiology, Clinical Presentation, and Treatment of Psoriasis: A Review. *JAMA* **2020**, *323*, 1945–1960. [CrossRef]
6. Simaljaková, M. Psoriasis—Etiopathogenesis, clinical picture and current therapy options. *Dermatol. Prax* **2008**, *2*, 50–55.
7. Lidaj, J.; Hegyi, V.; Danilla, T.; Masarovičová, A. PASI—Teória a prax. In *Péč J a kol. Chronická Ložisková Psoriáza, Komplexný Pohľad na Problematiku a Biologická liečba*; Dali-BB, s.r.o.: Banská Bystrica, Slovakia, 2006.
8. Ali, Z.; Zibert, J.R.; Dahiya, P.; Johansen, C.B.; Holm, J.G.; Jørgensen, A.-H.R.; Manole, I.; Suru, A.; Egeberg, A.; Thomsen, S.F.; et al. Mild-to-moderate severity of psoriasis may be assessed remotely based on photographs and self-reported extent of skin involvement. *JAAD Int.* **2023**, *11*, 129–136. [CrossRef]
9. Boehncke, W.-H.; Schön, M.P. Psoriasis. *Lancet* **2015**, *386*, 983–994. [CrossRef]
10. Braun-Falco, O.; Plewig, G.; Helmut, H.W. *Dermatology and Venereology*; Vydavatel'stvo Osveta: Martin, Slovakia, 2001.

11. Ali, F.; Neha, K.; Sharma, K.; Khasimbi, S.; Chauhan, G. Nanotechnology-based medicinal products and patents: A promising way to treat psoriasis. *Curr. Drug Deliv.* **2022**, *19*, 587–599. [CrossRef]
12. Guo, L.; Jin, H. Research progress of metabolomics in psoriasis. *Chin. Med. J.* **2023**, *2023*, 2504. [CrossRef]
13. Mascarenhas-Melo, F.; Carvalho, A.; Gonçalves, M.B.S.; Paiva-Santos, A.C.; Veiga, F. Nanocarriers for the topical treatment of psoriasis—Pathophysiology, conventional treatments, nanotechnology, regulatory and toxicology. *Eur. J. Pharm. Biopharm.* **2022**, *176*, 95–107. [CrossRef]
14. Gomes, G.S.; Frank, L.A.; Contri, R.V.; Longhi, M.S.; Pohlmann, A.R.; Guterres, S.S. Nanotechnology-based alternatives for the topical delivery of immunosuppressive agents in psoriasis. *Int. J. Pharm.* **2023**, *631*, 122535. [CrossRef]
15. Petit, R.G.; Cano, A.; Ortiz, A.; Espina, M.; Prat, J.; Muñoz, M.; Severino, P.; Souto, E.B.; García, M.L.; Pujol, M.; et al. Psoriasis: From Pathogenesis to Pharmacological and Nano-Technological-Based Therapeutics. *Int. J. Mol. Sci.* **2021**, *22*, 4983. [CrossRef]
16. Pradhan, M.; Alexander, A.; Singh, M.R.; Singh, D.; Saraf, S.; Saraf, S. Ajazuddin Understanding the prospective of nano-formulations towards the treatment of psoriasis. *Biomed. Pharmacother.* **2018**, *107*, 447–463. [CrossRef]
17. Shen, Q.; Liu, R.; Tan, S.; Xu, X.; Fang, J. Advances in pathogenesis and nanoparticles (NPs)-mediated treatment of psoriasis. *Front. Immunol.* **2022**, *13*, 1089262. [CrossRef]
18. Fereig, S.A.; El-Zaafarany, G.M.; Arafa, M.G.; Abdel-Mottaleb, M.M.A. Tackling the various classes of nano-therapeutics employed in topical therapy of psoriasis. *Drug Deliv.* **2020**, *27*, 662–680. [CrossRef]
19. Unna, P.G. Cignolin als Heilmittel der Psoriasis. *Derm. Wochenschr.* **1916**, *7*, 150–163.
20. Sehgal, V.N.; Verma, P.; Khurana, A. Anthralin/dithranol in dermatology. *Int. J. Dermatol.* **2014**, *53*, e449–e460. [CrossRef]
21. Ashton, R.E.; Andre, P.; Lowe, N.J.; Whitefield, M. Anthralin: Historical and current perspectives. *J. Am. Acad. Dermatol.* **1983**, *9*, 173–192. [CrossRef]
22. Seville, R. Advances in the use of anthralin. *J. Am. Acad. Dermatol.* **1981**, *5*, 319–321. [CrossRef]
23. Benezeder, T.; Gehad, A.; Patra, V.; Clark, R.; Wolf, P. Induction of IL-1β and antimicrobial peptides as a potential mechanism for topical dithranol. *Exp. Dermatol.* **2021**, *30*, 841–846. [CrossRef]
24. Behrangi, E.; Roohaninasab, M.; Sadeghzadeh-Bazargan, A.; Nobari, N.N.; Ghassemi, M.; Seirafianpour, F.; Goodarzi, A.; Dodangeh, M.; Md-Mph, M.D. A systematic review on the treatment of pediatric severe alopecia areata by topical immunotherapy or Anthralin (contact sensitization) or low-level light/laser therapy (LLLT): Focus on efficacy, safety, treatment duration, recurrence, and follow-up based on clinical studies. *J. Cosmet. Dermatol.* **2022**, *21*, 2727–2741. [CrossRef]
25. Painsi, C.; Patscheider, M.; Inzinger, M.; Huegel, R.; Lange-Asschenfeldt, B.; Quehenberger, F.; Wolf, P. Psoriasis Area and Severity Index 75 rate of classical inpatient dithranol therapy under daily life conditions. *Br. J. Dermatol.* **2015**, *173*, 815–817. [CrossRef]
26. Kadian, V.; Kumar, S.; Saini, K.; Kakkar, V.; Rao, R. Dithranol: An Insight into its Novel Delivery Cargos for Psoriasis Management. *Curr. Drug Res. Rev.* **2021**, *12*, 82–96. [CrossRef]
27. Kussini, J.; Charalambous, A.; Sachsenweger, F.; Steinert, M. Successful removal of anthralin staining from facial skin. *Int. J. Dermatol.* **2023**, *62*, e21–e22. [CrossRef]
28. Agrawal, U.; Mehra, N.K.; Gupta, U.; Jain, N.K. Hyperbranched dendritic nano-carriers for topical delivery of dithranol. *J. Drug Target.* **2013**, *21*, 497–506. [CrossRef]
29. Raza, K.; Katare, O.P.; Setia, A.; Bhatia, A.; Singh, B. Improved therapeutic performance of dithranol against psoriasis employing systematically optimized nanoemulsomes. *J. Microencapsul.* **2013**, *30*, 225–236. [CrossRef]
30. Sathe, P.; Saka, R.; Kommineni, N.; Raza, K.; Khan, W. Dithranol-loaded nanostructured lipid carrier-based gel ameliorate psoriasis in imiquimod-induced mice psoriatic plaque model. *Drug Dev. Ind. Pharm.* **2019**, *45*, 826–838. [CrossRef]
31. Nordin, U.U.M.; Ahmad, N.; Salim, N.; Yusof, N.S.M. Lipid-based nanoparticles for psoriasis treatment: A review on conventional treatments, recent works, and future prospects. *RSC Adv.* **2021**, *11*, 29080–29101. [CrossRef]
32. Hazari, S.A.; Kaur, H.; Karwasra, R.; Abourehab, M.A.; Khan, A.A.; Kesharwani, P. An overview of topical lipid-based and polymer-based nanocarriers for treatment of psoriasis. *Int. J. Pharm.* **2023**, *638*, 122938. [CrossRef]
33. Agarwal, R.; Katare, O.; Vyas, S. Preparation and in vitro evaluation of liposomal/niosomal delivery systems for antipsoriatic drug dithranol. *Int. J. Pharm.* **2001**, *228*, 43–52. [CrossRef]
34. Ahmad, M.Z.; Mohammed, A.A.; Algahtani, M.S.; Mishra, A.; Ahmad, J. Nanoscale Topical Pharmacotherapy in Management of Psoriasis: Contemporary Research and Scope. *J. Funct. Biomater.* **2022**, *14*, 19. [CrossRef]
35. de Mare, S.; Calis, N.; Hartog, G.D.; van Erp, P.; van de Kerkhof, P. The Relevance of Salicylic Acid in the Treatment of Plaque Psoriasis with Dithranol Creams. *Ski. Pharmacol. Physiol.* **1988**, *1*, 259–264. [CrossRef] [PubMed]
36. Hindson, C.; Diffey, B.; Lawlor, F.; Downey, A. Dithranol-UV-A phototherapy (DUVA) for psoriasis: A treatment without dressings. *Br. J. Dermatol.* **1983**, *108*, 457–460. [CrossRef]
37. Van De Kerkhof, P.; Van Der Valk, P.; Swinkels, O.; Kucharekova, M.; De Rie, M.; De Vries, H.; Damstra, R.; Oranje, A.; Spek, F.D.W.-V.d.; Van Neer, P.; et al. A comparison of twice-daily calcipotriol ointment with once-daily short-contact dithranol cream therapy: A randomized controlled trial of supervised treatment of psoriasis vulgaris in a day-care setting. *Br. J. Dermatol.* **2006**, *155*, 800–807. [CrossRef] [PubMed]
38. Fathalla, D.; Youssef, E.M.K.; Soliman, G.M. Liposomal and Ethosomal Gels for the Topical Delivery of Anthralin: Preparation, Comparative Evaluation and Clinical Assessment in Psoriatic Patients. *Pharmaceutics* **2020**, *12*, 446. [CrossRef] [PubMed]
39. Tokuyama, M.; Mabuchi, T. New Treatment Addressing the Pathogenesis of Psoriasis. *Int. J. Mol. Sci.* **2020**, *21*, 7488. [CrossRef] [PubMed]

40. Li, N.; Qin, Y.; Dai, D.; Wang, P.; Shi, M.; Gao, J.; Yang, J.; Xiao, W.; Song, P.; Xu, R. Transdermal Delivery of Therapeutic Compounds with Nanotechnological Approaches in Psoriasis. *Front. Bioeng. Biotechnol.* **2022**, *9*, 804415. [CrossRef]
41. Martínez-Ortega, L.; Mira, A.; Fernandez-Carvajal, A.; Mateo, C.R.; Mallavia, R.; Falco, A. Development of A New Delivery System Based on Drug-Loadable Electrospun Nanofibers for Psoriasis Treatment. *Pharmaceutics* **2019**, *11*, 14. [CrossRef]
42. Tomar, Y.; Pandit, N.; Priya, S.; Singhvi, G. Evolving Trends in Nanofibers for Topical Delivery of Therapeutics in Skin Disorders. *ACS Omega* **2023**, *8*, 18340–18357. [CrossRef]
43. Thakur, S.; Anjum, M.; Jaiswal, S.; Kumar, A.; Deepak, P.; Anand, S.; Singh, S.; Rajinikanth, P.S. Novel Synergistic Approach: Tazarotene-Calcipotriol-Loaded-PVA/PVP-Nanofibers Incorporated in Hydrogel Film for Management and Treatment of Psoriasis. *Mol. Pharm.* **2023**, *20*, 997–1014. [CrossRef]
44. Andrýsková, N.; Sourivong, P.; Babincová, M.; Šimaljaková, M. Controlled Release of Tazarotene from Magnetically Responsive Nanofiber Patch: Towards More Efficient Topical Therapy of Psoriasis. *Appl. Sci.* **2021**, *11*, 11022. [CrossRef]
45. Babinec, P.; Jirsák, O. Microwave absorbing nonwoven textile from electrospun magnetically responsive nano-fibers. *Optoelectron. Adv. Mat.* **2008**, *2*, 474–477.
46. Babincová, N.; Jirsák, O.; Babincová, M.; Babinec, P.; Šimaljaková, M. Remote magnetically controlled drug release from electrospun composite nanofibers: Design of a smart platform for therapy of psoriasis. *Z. Naturforsch.* **2020**, *75*, 587–591. [CrossRef]
47. Khoshbakht, S.; Asghari-Sana, F.; Fathi-Azarbayjani, A.; Sharifi, Y. Fabrication and characterization of tretinoin-loaded nanofiber for topical skin delivery. *Biomater. Res.* **2020**, *24*, 8. [CrossRef] [PubMed]
48. Pant, B.; Park, M.; Park, S.-J. Drug Delivery Applications of Core-Sheath Nanofibers Prepared by Coaxial Electrospinning: A Review. *Pharmaceutics* **2019**, *11*, 305. [CrossRef]
49. Elyaderani, A.K.; Lama-Odría, M.d.C.D.; del Valle, L.J.; Puiggalí, J. Multifunctional Scaffolds Based on Emulsion and Coaxial Electrospinning Incorporation of Hydroxyapatite for Bone Tissue Regeneration. *Int. J. Mol. Sci.* **2022**, *23*, 15016. [CrossRef]
50. Nadaf, A.; Gupta, A.; Hasan, N.; Fauziya; Ahmad, S.; Kesharwani, P.; Ahmad, F.J. Recent update on electrospinning and electrospun nanofibers: Current trends and their applications. *RSC Adv.* **2022**, *12*, 23808–23828. [CrossRef]
51. Yang, Y.; Chen, W.; Wang, M.; Shen, J.; Tang, Z.; Qin, Y.; Yu, D.-G. Engineered Shellac Beads-on-the-String Fibers Using Triaxial Electrospinning for Improved Colon-Targeted Drug Delivery. *Polymers* **2023**, *15*, 2237. [CrossRef]
52. Furukawa, S.; Nagamatsu, A.; Nenoi, M.; Fujimori, A.; Kakinuma, S.; Katsube, T.; Wang, B.; Tsuruoka, C.; Shirai, T.; Nakamura, A.J.; et al. Space Radiation Biology for "Living in Space". *BioMed Res. Int.* **2020**, *2020*, 4703286. [CrossRef]
53. Bernhard, G.H.; Bais, A.F.; Aucamp, P.J.; Klekociuk, A.R.; Liley, J.B.; McKenzie, R.L. Stratospheric ozone, UV radiation, and climate interactions. *Photochem. Photobiol. Sci.* **2023**, *22*, 937–989. [CrossRef]
54. Anaya-Esparza, L.M.; Ruvalcaba-Gómez, J.M.; Maytorena-Verdugo, C.I.; González-Silva, N.; Romero-Toledo, R.; Aguilera-Aguirre, S.; Pérez-Larios, A.; Montalvo-González, E. Chitosan-TiO_2: A Versatile Hybrid Composite. *Materials* **2020**, *13*, 811. [CrossRef]
55. Schneider, S.L.; Lim, H.W. A review of inorganic UV filters zinc oxide and titanium dioxide. *Photodermatol. Photoimmunol. Photomed.* **2019**, *35*, 442–446. [CrossRef] [PubMed]
56. Wiśniewski, M.; Roszek, K. Underestimated Properties of Nanosized Amorphous Titanium Dioxide. *Int. J. Mol. Sci.* **2022**, *23*, 2460. [CrossRef] [PubMed]
57. Jiang, Y.; Dong, K.; An, J.; Liang, F.; Yi, J.; Peng, X.; Ning, C.; Ye, C.; Wang, Z.L. UV-Protective, Self-Cleaning, and Antibacterial Nanofiber-Based Triboelectric Nanogenerators for Self-Powered Human Motion Monitoring. *ACS Appl. Mater. Interfaces* **2021**, *13*, 11205–11214. [CrossRef] [PubMed]
58. Koozekonan, A.G.; Esmaeilpour, M.R.M.; Kalantary, S.; Karimi, A.; Azam, K.; Golbabaei, F. Fabrication and characterization of TiO2 and MWCNT coated electrospinning nanofibers for UV protection properties. *Methodsx* **2021**, *8*, 101354. [CrossRef]
59. Hedayatnasab, Z.; Dabbagh, A.; Abnisa, F.; Wan Daud, W.M.A. Polycaprolactone-coated superparamagnetic iron oxide nanoparticles for in vitro magnetic hyperthermia therapy of cancer. *Eur. Polym. J.* **2020**, *133*, 109789. [CrossRef]
60. Available online: https://imagetool.software.informer.com/3.0/ (accessed on 19 March 2017).
61. Thoma, K.; Holzmann, C. Photostability of dithranol. *Eur. J. Pharm. Biopharm.* **1998**, *46*, 201–208. [CrossRef]
62. Savian, A.L.; Rodrigues, D.; Weber, J.; Ribeiro, R.F.; Motta, M.H.; Schaffazick, S.R.; Adams, A.I.; de Andrade, D.F.; Beck, R.C.; da Silva, C.B. Dithranol-loaded lipid-core nanocapsules improve the photostability and reduce the in vitro irritation potential of this drug. *Mater. Sci. Eng. C* **2015**, *46*, 69–76. [CrossRef]
63. Melo, T.S.E.; Dubertret, L.; Prognon, P.; Gond, A.; Mahuzier, G.; Santus, R. Physicochemical Properties and Stability of Anthralin in Model Systems and Human Skin. *J. Investig. Dermatol.* **1983**, *80*, 1–6. [CrossRef]
64. Mahrle, G.; Bonnekoh, B.; Ghyczy, M.; Wiegrebe, W. Stability of anthralin in liposomal phospholipids. *Arch. Dermatol. Res.* **1991**, *283*, 483–484. [CrossRef]
65. Herman, J.; Remon, J.; De Bersaques, J. Influence of storage conditions on the stability of anthralin in the presence of coal tar and salicylic acid in a white soft paraffin base. *J. Am. Acad. Dermatol.* **1988**, *18*, 750–751. [CrossRef]
66. Babincová, M. Microwave induced likage of magnetoliposomes. Possible clinical implications. *Bioelectrochemistry Bioenerg.* **1993**, *32*, 187–189. [CrossRef]

67. Babincová, M.; Vrbovská, H.; Sourivong, P.; Babinec, P.; Durdík, Š. Application of Albumin-embedded Magnetic Nanoheaters for Release of Etoposide in Integrated Chemotherapy and Hyperthermia of U87-MG Glioma Cells. *Anticancer. Res.* **2018**, *38*, 2683–2690. [CrossRef] [PubMed]
68. Caizer, C. Optimization Study on Specific Loss Power in Superparamagnetic Hyperthermia with Magnetite Nanoparticles for High Efficiency in Alternative Cancer Therapy. *Nanomaterials* **2020**, *11*, 40. [CrossRef] [PubMed]
69. Zahn, D.; Landers, J.; Buchwald, J.; Diegel, M.; Salamon, S.; Müller, R.; Köhler, M.; Ecke, G.; Wende, H.; Dutz, S. Ferrimagnetic Large Single Domain Iron Oxide Nanoparticles for Hyperthermia Applications. *Nanomaterials* **2022**, *12*, 343. [CrossRef]
70. Dutz, S.; Hergt, R. Magnetic nanoparticle heating and heat transfer on a microscale: Basic principles, realities and physical limitations of hyperthermia for tumour therapy. *Int. J. Hyperthermia* **2013**, *29*, 790–800. [CrossRef]
71. Babincová, N.; Sourivong, P.; Babinec, P.; Bergemann, C.; Babincová, M.; Durdík, Š. Applications of magnetoliposomes with encapsulated doxorubicin for integrated chemotherapy and hyperthermia of rat C6 glioma. *Z. Naturforsch. C* **2018**, *73*, 265–271. [CrossRef]
72. Niiyama, E.; Uto, K.; Lee, C.M.; Sakura, K.; Ebara, M. Alternating Magnetic Field-Triggered Switchable Nanofiber Mesh for Cancer Thermo-Chemotherapy. *Polymers* **2018**, *10*, 1018. [CrossRef]
73. Boraei, S.B.A.; Nourmohammadi, J.; Bakhshandeh, B.; Dehghan, M.M.; Gholami, H.; Gonzalez, Z.; Sanchez-Herencia, A.J.; Ferrari, B. Capability of core-sheath polyvinyl alcohol–polycaprolactone emulsion electrospun nanofibrous scaffolds in releasing strontium ranelate for bone regeneration. *Biomed. Mater.* **2021**, *16*, 25009. [CrossRef]
74. Zhu, X.; Ni, S.; Xia, T.; Yao, Q.; Li, H.; Wang, B.; Wang, J.; Li, X.; Su, W. Anti-Neoplastic Cytotoxicity of SN-38-Loaded PCL/Gelatin Electrospun Composite Nanofiber Scaffolds against Human Glioblastoma Cells In Vitro. *J. Pharm. Sci.* **2015**, *104*, 4345–4354. [CrossRef]
75. Dias, J.R.; Sousa, A.; Augusto, A.; Bártolo, P.J.; Granja, P.L. Electrospun Polycaprolactone (PCL) Degradation: An In Vitro and In Vivo Study. *Polymers* **2022**, *14*, 3397. [CrossRef]
76. Yilmaz, C.N.C.; Pamfil, D.; Vasile, C.; Bibire, N.; Lupuşoru, R.-V.; Zamfir, C.-L.; Lupușoru, C.E. Toxicity, Biocompatibility, pH-Responsiveness and Methotrexate Release from PVA/Hyaluronic Acid Cryogels for Psoriasis Therapy. *Polymers* **2017**, *9*, 123. [CrossRef] [PubMed]
77. Malašauskiene, J.; Milašius, R.; Kuchanauskaitė, E. Possibilities for the Estimation of Electrospun Nanofibre Diameter Distribution by Normal (Gaussian) Distribution. *Fibres Text. East. Eur.* **2016**, *24*, 23–28. [CrossRef]
78. Mikhaylova, M.; Kim, D.K.; Bobrysheva, N.; Osmolowsky, M.; Semenov, V.; Tsakalakos, T.; Muhammed, M. Superparamagnetism of Magnetite Nanoparticles: Dependence on Surface Modification. *Langmuir* **2004**, *20*, 2472–2477. [CrossRef] [PubMed]
79. Boreham, D.R.; Gasmann, H.C.; Mitchel, R.E.J. Water bath hyperthermia is a simple therapy for psoriasis and also stimulates skin tanning in response to sunlight. *Int. J. Hyperth.* **1995**, *11*, 745–754. [CrossRef] [PubMed]